Mass Spectrometry of Laser-Initiated Carbene Reactions for Protein Topographic Analysis

ARTICLE *in* ANALYTICAL CHEMISTRY · MARCH 2011

Impact Factor: 5.64 · DOI: 10.1021/ac102655f · Source: PubMed

2 AUTHORS:

Chanelle C Jumper
University of Toronto
9 PUBLICATIONS **49** CITATIONS
SEE PROFILE

David C Schriemer
The University of Calgary
92 PUBLICATIONS **2,390** CITATIONS
SEE PROFILE

analytical chemistry

ARTICLE

pubs.acs.org/ac

Mass Spectrometry of Laser-Initiated Carbene Reactions for Protein Topographic Analysis

Chanelle C. Jumper[†] and David C. Schriemer[†,‡,*]

[†]Departments of Chemistry and [‡]Biochemistry & Molecular Biology, University of Calgary, Calgary, Alberta, T2N 1N4, Canada

Supporting Information

ABSTRACT: We report a protein labeling method using nonselective carbene reactions of sufficiently high efficiency to permit detection by mass spectrometric methods. The approach uses a diazirine-modified amino acid (L-2-amino-4,4′-azipentanoic acid, "photoleucine") as a label source, which is converted to a highly reactive carbene by pulsed laser photolysis at 355 nm. Labeling of standard proteins and peptides (CaM, Mb, M13) was achieved with yields up to 390-fold higher than previous studies using methylene. Carbene labeling is sensitive to changes in protein topography brought about by conformational change and ligand binding. The modification of apo-CaM was 45 ± 7% higher than that of holo-CaM. Modification of the CaM-M13 complex reflected a 39 ± 1% reduction in labeling for bound holo-CaM relative to free holo-CaM. Labeling yield is independent of protein concentration over approximately 2 orders of magnitude but is weakly dependent on the presence of other chromophores in a photon-limited apparatus. The current configuration required 2 min of irradiation for full reagent conversion; however, it is shown that comparable yields can be achieved with a single high-energy laser pulse (>100 mJ/pulse, <10 ns), offering a labeling method with high temporal resolution. We suggest a mechanism of labeling governed by limited carbene diffusion and the protein surface activity of the diazirine precursor. This surface activity is speculated to return a measure of selectivity relative to methylene labeling, which ultimately may be tunable.

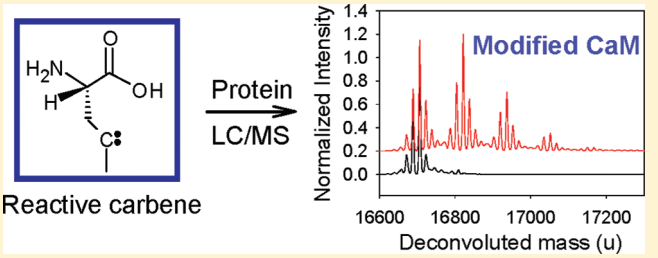

The close relationship between protein structure and function fuels ongoing research in method development for structural characterization of proteins and their interactions. X-ray crystallography and nuclear magnetic resonance (NMR) spectroscopy are well-established tools for such applications but present fundamental limitations related to crystallization, molecular weight, solubility, and concentration. Methods in structural mass spectrometry (MS) provide a useful supplement by providing topographical data that can be mined for structure-building and characterizing protein conformational change, particularly for systems involving large protein complexes and their interactions.[1,2]

Such data can be obtained from differential chemical labeling experiments.[3] Altered rates of labeling can reflect changes in the exposure of the protein, depending on the mechanism of the labeling chemistry. Changes in surface exposure can be probed by examining the permanent or temporary bonds formed from reactions of the protein with chemical reagents. The location of the modifications can be mapped down to the peptide level by proteolytic digestion prior to analysis. Mass spectrometry is well-suited for detecting and quantifying modified proteins and peptides, since the modifications result in a mass shift that can be accurately detected with high sensitivity and speed, while tandem MS offers possibilities for residue-level resolution. For example, hydrogen/deuterium exchange (H/DX)−MS has been used extensively for probing protein structure and dynamics.[4−7] With the exception of amide bonds N-terminal to proline residues, exchange is not limited to specific backbone amides and therefore offers a relatively unbiased view of protein topography. The spatial resolution may be limited to the peptide level by H/D for most practical applications, as a result of hydrogen scrambling in the gas phase upon collisionally induced dissociation. However, recent efforts using electron-transfer or electron-capture dissociation on "cool" ions show some promise in locating amide hydrogens, particularly for small intact proteins.[8−11] Nevertheless, the temporal constraints imposed by amide hydrogen back-exchange limit H/DX-MS to protein systems of modest complexity.

Stable covalent labels that do not back-exchange or scramble offer a solution to these limitations. Chemical reagents leading to the modification of specific amino acids such as lysine, cysteine, and tyrosine[12−14] have some utility; however, selective labeling does not probe the topography of an entire protein or complex. Numerous targeted labeling methods have been recently reviewed by Mendoza and Vachet.[15] Methods that modify a wider range of amino acids provide a better representation of the overall surface area. For example, diethyl pyrocarbonate can probe up to 25% of protein sequence.[16] Hydroxyl radical labeling improves upon this representation, as it can modify the side

Received: November 4, 2010
Accepted: February 25, 2011
Published: March 22, 2011

chains of any oxidizable amino acid.[17,18] Although this includes the majority of amino acids, labeling rates vary considerably.[19,20] Two complications with oxidative labeling have been reported, namely a protein concentration dependence observed with γ-ray mediated labeling[21] (which is likely present in other sources for the ·OH label) and variable yields resulting from solution additives acting as radical scavengers.[22]

A final consideration is the temporal resolution of a labeling method, which depends on the rate of the labeling reaction and the rate of generation for reactive species. If reagent exposure is reduced to a time-scale below that of a protein conformational change, then the modification reaction may be used to follow its kinetics, which has implications for understanding the effects of dynamics on biochemical processes. To date, hydroxyl radicals offer the shortest exposure by using a pulsed laser for generation, and reducing ·OH lifetimes to ~1 μs by scavenging persistent radicals with additives.[23,24] These fast photochemical oxidations of protein (FPOP) experiments offer a slight amino acid "tuning capacity" as well, based on the source of radical anion used.[25]

There remains room for an improved labeling strategy. The ideal covalent reagent would rapidly and irreversibly probe the entire protein surface and be independent of the chemical properties of the accessible residues. It would be nonreactive toward the protein prior to activation. Further, labeling would be independent of protein concentration within a range, tolerant of varying solution conditions, and impart mass shifts that are easily resolved from native modifications. One labeling chemistry that may fulfill these objectives involves the singlet carbene generated from the photolysis of a diazirine functional group, which is otherwise chemically inert.[26,27] Carbenes are appealing as chemical labeling reagents, as they appear to probe all amino acids,[28] providing nonselective chemical modification. Singlet carbenes may also permit sub-microsecond labeling due to their short lifetime in solvent, on the order of nanoseconds.[29]

Use of diazirine gas (CH_2N_2) as a methylene source for chemical footprinting was introduced in 2000 by Richards et al.[28] but has received limited attention since then.[30−33] Diazirine gas is characterized by low solubility, and, as such, the level of labeling is limited by available reagent in the solution.[34] Only low levels of labeling could be achieved, on the order of 6×10^{-7} labels/Å^2 for folded proteins (e.g., 4×10^{-3} labels per molecule of α-lactalbumin).[32] Detection of modified protein has been limited to scintillation counting of tritiated methylene following long workup procedures. Prospects for reliable mass spectrometric detection are limited with this particular method, which is likely the reason for low interest in this type of labeling. In addition, the use of an explosive reagent gas requires on-site vacuum line synthesis and careful storage.

In this study, we describe a method for carbene labeling demonstrating product yields detectable within the dynamic range of the mass spectrometer. A stable diazirine-modified leucine isostere is explored as a potential labeling reagent with the advantage of higher water solubility and stability, which eliminates the need to synthesize on-site. The labeling reaction is characterized and evaluated at the protein level for the detection of conformational changes and binding events. The mechanisms, opportunities, and current limitations of this approach are discussed.

EXPERIMENTAL SECTION

Materials. L-Photoleucine was obtained from Thermo Scientific (Rockford, IL). Lyophilized calmodulin (CaM) was provided by Dr. Hans Vogel in the department of Biological Sciences at the University of Calgary (Calgary, AB). Equine skeletal muscle myoglobin (Mb), myosin light chain kinase peptide (M13), tris(hydroxymethyl)aminomethane (Tris), urea, formic acid, potassium chloride, hydrochloric acid, sodium hydroxide, and calcium chloride were obtained from Sigma Aldrich (St. Louis, MO). EDTA disodium salt was obtained from Amersham Pharmacia Biotech (Uppsala, Sweden). HPLC water and HPLC acetonitrile were obtained from Fisher Scientific (Fair Lawn, NJ).

Carbene Reactions. Protein (Mb, CaM, M13, or CaM-M13 complex) was equilibrated for 15 min at 10 μM with 100 mM photoleucine in 10 mM Tris buffer (100 mM KCl, pH 7.5) and 1 mM $CaCl_2$ or 5 mM EDTA in the cases of holo- and apo-CaM, respectively. A 2 μL aliquot was placed in a well of a 96-well plate (Agilent Technologies, Denmark). Covalent modification was initiated by photolysis of photoleucine using the third harmonic of a Nd:YAG pulsed laser (355 nm, 1000 Hz, 12.9 μJ/pulse) from an oMALDI source of an AB Sciex QSTAR XL mass spectrometer. The beam was focused on the droplet through a slit in the plate lid, and varying irradiation times were investigated, in triplicate. Samples were diluted to 1 μM with an aqueous solution containing 0.2% formic acid and 3% acetonitrile, prior to chromatographic analysis. Photolysis products were monitored in the absence of protein by irradiating 100 mM photoleucine in water followed by dilution to 100 μM in 50:50 acetonitrile containing 2.5 μM glutamine as an internal standard. For higher-energy laser experiments, carbene labeling of holo-CaM was initiated by single-pulse photolysis using a Nd:YAG laser (20−100 mJ/pulse, pulse width of 8−10 ns fwhm, Spectra Physics).

HPLC Analysis. An 1100 series (Agilent, Wilmington, DE) HPLC system with a C4 column (500 μM i.d. × 5 mm, 5 μm particle size, Dionex, Sunnyvale, CA) was used for sample desalting and separation. Proteins and/or peptides were eluted using a gradient of acetonitrile containing 0.2% formic acid that increased from 3 to 80% over 15 min at a flow rate of 50 μL/min. Photoleucine photolysis products (in the absence of protein) were analyzed by direct infusion at a flow rate of 10 μL/min.

Mass Spectrometry. Mass spectra were acquired in TOF-MS mode on an AB Sciex (Foster City, CA) QSTAR XL quadrupole time-of-flight mass spectrometer equipped with a turbo electrospray ionization source, with nebulization (spray voltage of 5 kV and desolvation temperature of 200 °C). Protein spectra were acquired in positive ion mode. Photoleucine spectra were acquired under similar conditions.

Data Analysis. Extent of modification is expressed in units of average number of labels per protein molecule or equivalently, average mol label/mol protein. This is calculated by determining the difference in the number average molecular weight (that is, the centroided mass) between the labeled and unlabeled protein from deconvolved spectra:

$$\Delta\text{mass}_{\text{av}} = \left[\frac{\Sigma m_i I_i}{\Sigma I_i}\right]_{\text{labeled}} - M_{\text{unlabeled}} \qquad (1)$$

where m_i and I_i represent the mass and intensity, respectively, of the protein "mass signature" shifted by the inclusion of i carbene labels. The mass signature is the distribution of solvent adducts, oxidation products, and neutral loss products of a given carbene incorporation level. Here, m_i is simply the mass of the unmodified ith peak, and I_i is the summed intensity of the unmodified form and all adducts, oxidation products, and neutral loss

products for that signature. This approach is required as the mass signatures can vary slightly between labeled and unlabeled species. $M_{unlabeled}$ is the average mass of the unlabeled, unmodified protein. The overall mass change upon labeling divided by the mass of a single modification (115.13 u) gives the average number of labels added per protein molecule.

Determination of Solvent Accessibility. Solvent accessibility was calculated from Protein Data Bank (PDB) coordinate files using the program MSMS.[35] The PDB files selected were 1DWR for Mb, 1LKJ for apo-CaM, 1PRW for holo-CaM, 2OSG for CaM-M13 complex, and 2KOF for M13. A probe radius of 1.4 Å was used, representing the van der Waals radius of water. Increasing probe radii (1−2.5 Å) were also investigated to examine "reagent-accessible" surface area.

H/DX-MS. Hydrogen−deuterium exchange labeling was investigated for holo-CaM and Mb at all irradiation time points. Carbene labeling was carried out as described followed by the immediate addition of 50% D_2O for 2.5 min at 20 °C. Deuterium labeling was quenched by the addition of cold aqueous solution containing 0.2% formic acid and 3% acetonitrile, followed by LC-MS analysis as described, but under cold conditions (∼0 °C). The solvents and the chromatographic column were kept on ice, while the samples were loaded from a refrigerated autosampler at 4 °C. Total analysis time for each sample was 13 min from quenching.

RESULTS AND DISCUSSION

Principle of Labeling. Photoleucine, a stable diazirine-based leucine mimic, was used as the labeling reagent in this study. Laser photolysis of photoleucine liberates nitrogen, yielding a highly reactive singlet carbene, capable of reacting with its immediate molecular cage.[27] The lifetime of this carbene is expected to be on the nanosecond time-scale based on studies of related structures,[29] with corresponding reaction rates approaching the diffusion limit.[36] Carbene chemistry involves direct insertion into any X-H bond (including saturated hydrocarbons) or addition to a double bond (including unsaturated hydrocarbons and aromatics).[26] As such, the reagent is capable of probing every amino acid in a protein (see Figure S1 in Supporting Information).[27] However, internal conversion and reaction with water represent the most likely reaction products.

To determine conversion efficiency and product distribution in bulk solvent, we first irradiated photoleucine in the absence of protein. Shown in Figure S2 in Supporting Information are the levels of alcohol and alkene products from the photolysis of the carbene in water, as a function of irradiation time. Since the reaction is essentially immediate, the rates of alcohol and alkene formation are an indicator of conversion efficiency for photoleucine to the corresponding carbene. High reaction rates preclude any persistent reactivity of the carbene. This unimolecular conversion follows pseudo-first -order kinetics on the basis of available energy, being nearly complete within 2 min of irradiation in the apparatus we used.

In the presence of protein, photolysis is expected to label a fraction of amino acids at the reagent-accessible surface of the protein. Figure 1 shows the spectra for the reaction products of myoglobin (Mb) and holo-calmodulin (CaM). Each reaction product is offset by 115.13 u, the average mass of a single modification. The level of modification is reproducible within a fixed set of solution conditions, with a typical relative standard deviation of ±5%.

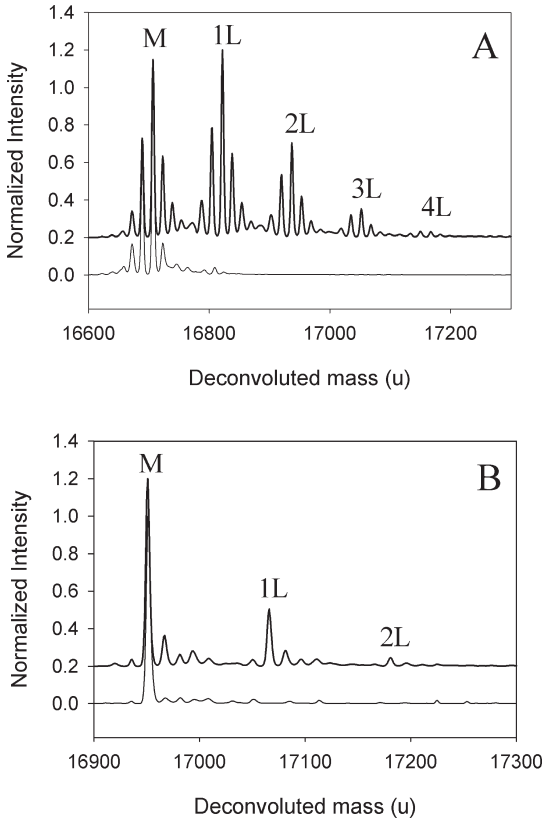

Figure 1. Deconvoluted mass spectra of labeled and unlabeled (A) Mb and (B) holo-calmodulin. Product distributions annotated according to unlabeled protein (M) and labeled protein (*x*L), where annotations refer to the " mass signature" consisting of the adducts, oxidation products, and neutral loss products for a given label incorporation level. Labeled product spectra are vertically offset by 0.2 for comparison. Label data represent photolysis for 6 min in 100 mM photoleucine.

A number of controls validate this reaction. First, the addition of photoleucine to the protein samples in the absence of laser activation resulted in no detectable labeling products, compared to the isolated protein. Second, since the photolysis product from internal conversion of photoleucine has a mass of 115.13 u (equivalent to the mass of a modification), noncovalent adduction of the alkene to the protein could occur. To test this, photoleucine photolysis products were generated in isolation and then mixed with protein, followed by MS analysis. No detectable adduction products were present compared to the isolated protein. Third, protein tertiary structure may change during photolysis that is 2 min in duration. We irradiated the protein solutions in the absence of diazirine for 20 min, followed by labeling for 2 min. The level of modification did not vary significantly from the control.

Evaluating Reaction Yield. The average number of modifications per protein molecule was calculated to describe the extent of modification, following the approach by Delfino et al.[30−32] This method assumes that protein ionization efficiency is not affected upon modification, which seems reasonable here. The extent of modification was examined for holo-CaM as a function of irradiation time (Figure 2). Modification levels plateau at ∼2 min as expected based on the kinetics of reagent depletion (Figure S2 in Supporting Information). In a collisional model, if reagent collides with protein and is coincident with the photolytic event, a

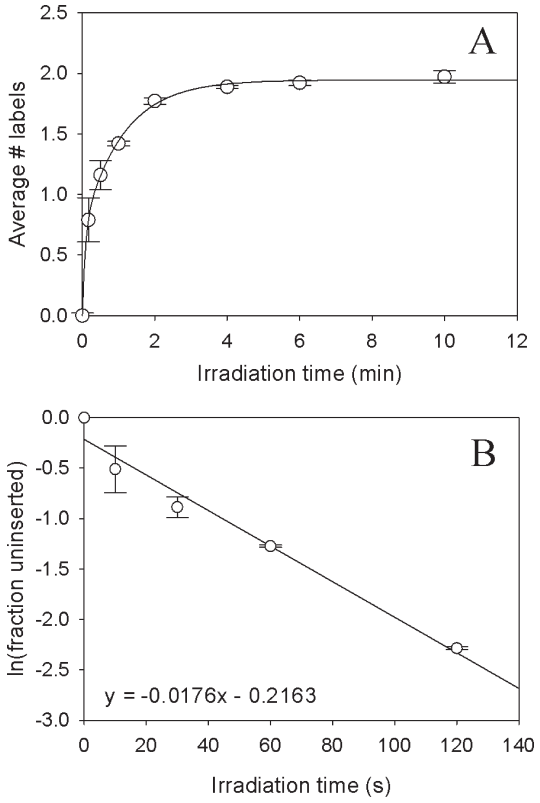

Figure 2. Kinetics of protein labeling in the current photolysis system. (A) Extent of holo-calmodulin labeling in Tris buffer expressed as the number average labeling (eq 1) as a function of irradiation time. (B) Data as in A, shown as a ln plot of the fraction of "uninserted" carbene ($1 - [B_t]/[B_{max}]$), and fit accordingly. Inset equation represents the linear fit following eq 3. Data generated from irradiation of 10 μM calmodulin in 100 mM photoleucine. All points represent triplicate analyses with error bars $\pm$1 SD.

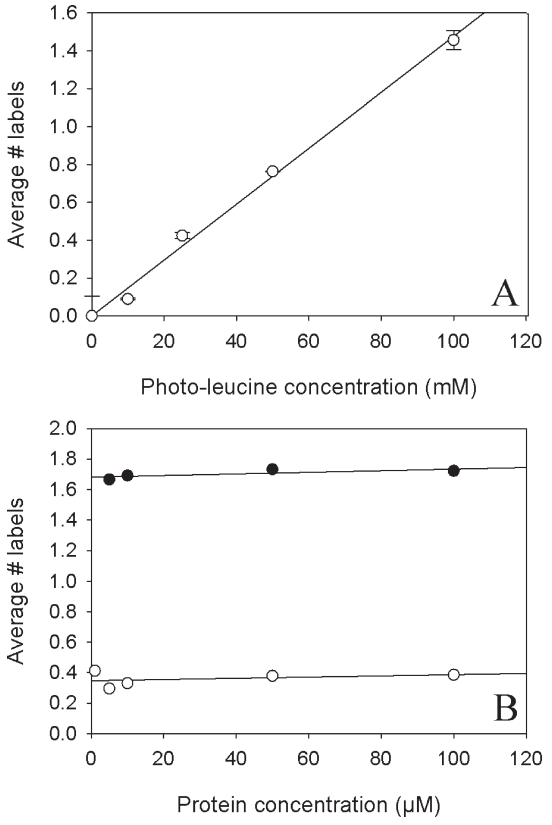

Figure 3. Evaluating the model of carbene labeling when using photoleucine. (A) Determination of labeling dependency on reagent concentration. Holo-calmodulin labeling yield is expressed as a function of photoleucine concentration, where labeling is measured at saturation. All points represent triplicate analyses with error bars $\pm$1 SD (B) Determination of labeling dependency on protein concentration and surface area. Labeling yield at saturation for holo-calmodulin (closed circles) and Mb (open circles), expressed as a function of protein concentration. Experiment conducted with 100 mM photoleucine. Lines represent fits for visual clarity.

successful labeling event can result. For a given protein−solvent system, this permits description by a simple unimolecular reaction,

$$\mathrm{A} \xrightarrow{h\nu} \mathrm{B} \qquad (2)$$

where A is photoleucine in the molecular cage around the protein available for reaction, and B is the protein-quenched carbene in the cage region, produced upon photolysis. Partitioning of photoleucine from bulk solvent into the molecular cage during irradiation can be ignored, as the photolysis rates for bulk vs surface photoleucine should be identical. Pseudo-first-order kinetics are appropriate for this reaction,

$$\ln\left(1 - \frac{[B_t]}{[B_{max}]}\right) = -kt \qquad (3)$$

where $[B_t] = [A_t - A_0]$, the concentration of protein-quenched carbene generated after time t, and $[B_{max}] = [A_0]$, the maximum concentration of protein-quenched carbene generated, which depends on the initial diazirine concentration in the molecular cage. $[B_t]/[B_{max}]$ is determined experimentally from the average number of protein labels at t normalized to the maximum number of labels. A plot of labeling data rendered in this fashion was fit to a straight line, yielding a k of 0.018 s^{-1} (Figure 2b). This conversion rate is comparable to that generated for a solvent-quenched reaction (Figure S2 in Supporting Information).

Modifying the quantification approach by Craig et al.,[30] the maximum reaction yield can be approximated as

$$\text{max. average yield} = C\left(\frac{SA_{protein}[protein]}{SA_{water}[water]}\right)\left(\frac{[diazirine]}{[protein]}\right) \qquad (4)$$

which may be simplified to

$$\text{max. average yield} = C'(SA_{protein}[diazirine]) \qquad (5)$$

In eq 4, $SA_{protein}$ and SA_{water} represent the surface area of the protein and water, respectively. The first bracketed expression in this equation reflects the probability of a single protein labeling event based on geometrical considerations, where the second reflects the amount of carbene available for a given protein molecule and assumes that all free diazirine is converted to the reactive carbene.[32] Here, C is a factor inserted to aid in quantitating global deviations from the model, where we note that $C = 1$ provides a good fit for labeling experiments of folded proteins using diazirine gas.[32] Certain assumptions have been

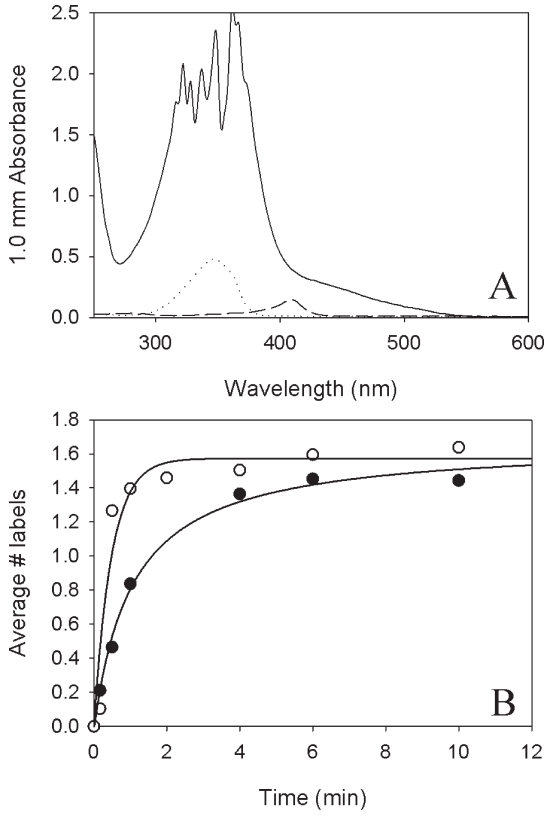

Figure 4. Effect of competitive absorption on carbene labeling yield. (A) Absorption spectra of 10 μM Mb (large dashed line), 100 mM L-photoleucine (dotted line), and 100 μM HABA (solid line). Kinetics of holo-calmodulin labeling in Tris buffer in the presence (closed circles) and absence (open circles) of 100 μM HABA. Lines represent fits for visual clarity.

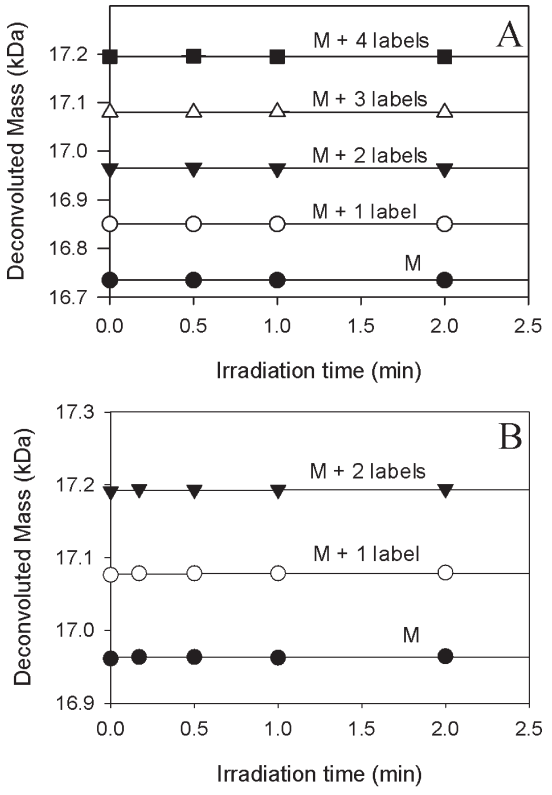

Figure 5. Determining the influence of carbene modifications on the stability of (A) calmodulin and (B) myoglobin. Data represents deuterated protein masses from H/DX-MS experiments of individual photolysis products as a function of time, where photolysis products are indicated as residual unlabeled protein (M) or as labeled protein with X labels (M+X). All experiments used 10 μM protein in Tris buffer. Linear fits have slopes of zero, within error.

applied to generate this simple formalism. We assume the labeling reaction is isotropic and thus not dependent on the orientation of the reactants, a true "billiard ball" model. We also ignore (a) the possibility of saturating the protein surface with label and (b) polymerization of the carbene. These should be reasonable assumptions, as water (55 M) competes with protein (10 μM) for carbene. We then set out to test the simplified model of eq 5.

CaM labeling does indeed increase proportionally with reagent concentration (Figure 3a), using an irradiation time sufficient to ensure complete reagent conversion (2 min). Labeling is also independent of protein concentration over 1−100 μM for both holo-CaM and Mb (Figure 3b). At a given diazirine concentration, labeling yield should be proportional to protein surface area if the previous work with diazirine gas is any indication, but this correlation does not seem strong, at least based on the two proteins we studied (Figure 3b). To compare our results with methylene labeling, we assume a solvent-accessible surface area (SASA) of 8200 Å^2 for holo-CaM and 8050 Å^2 for Mb, along with a labeling yield of 6×10^{-7} labels per Å^2. The latter value arises from methylene labeling of folded proteins, where the correlation with SASA is good.[32] Based on these values, the yield we measure for holo-CaM labeling is 390 times greater than would be expected for methylene labeling of folded holo-CaM. The yield for Mb is 60 times greater.

The basis for these increases can be better understood with the aid of eq 4, which assumes a simple surface accessibility model. The 100-fold increase in diazirine concentration over diazirine gas drives much of this but also clearly highlights departures from the model. Here, holo-CaM results in a C of 3.2 and Mb a C of 0.6, using a spherical model of water of radius 1.4 Å, water at 55.5 M, protein surface area of 8000 Å^2, and a diazirine concentration of 0.100 M. These deviations from C of 1 appear to reflect the protein "surface activity" of photoleucine relative to diazirine gas: holo-CaM appears to have a greater affinity for photoleucine than for diazirine gas, while Mb has a somewhat reduced affinity for photoleucine. This has implications for the overall selectivity of this particular diazirine probe. Further evidence for surface activity will be presented and discussed below. Here, we simply note that the net increase in yield for both proteins provides an opportunity to test for differential labeling when global transitions occur in protein systems.

Competitive Absorption. In the presence of solution components that absorb at 355 nM, rates of carbene generation should be reduced. As this has considerable practical significance when selecting buffer conditions, we tested the effect of 4-hydroxyazobenzoic acid (HABA) on labeling yield for holo-CaM. HABA strongly absorbs at 355 nm (Figure 4a). In the current configuration of our photolysis system, this simply delays maximum labeling as expected but does not influence maximum labeling levels (Figure 4b). However, when the intensity of the light source is limiting, optical transparency must be taken into consideration.

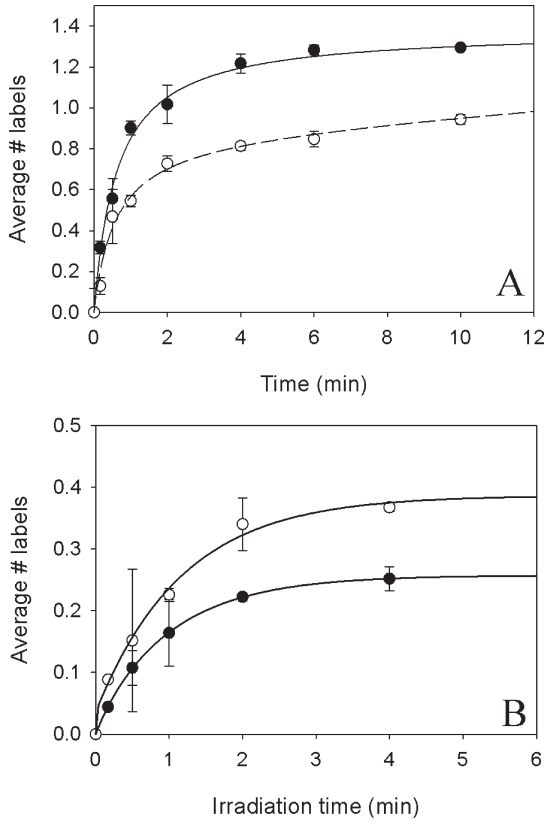

Figure 6. Determining the sensitivity of carbene labeling to protein conformational changes. (A) Ca^{2+}-induced conformational change on calmodulin where apo-calmodulin (closed circles) and holo-calmodulin (open circles) were labeled with 100 mM photoleucine in phosphate buffer and monitored as function of time. (B) Myoglobin conformational change resulting from heme extraction with 2-butanone, where heme-free myoglobin (open circles) and heme-bound myoglobin (closed circles) were both labeled in 100 mM photoleucine in Tris buffer. Error bars represent ±1 SD from triplicate analyses. Lines represent fits for visual clarity.

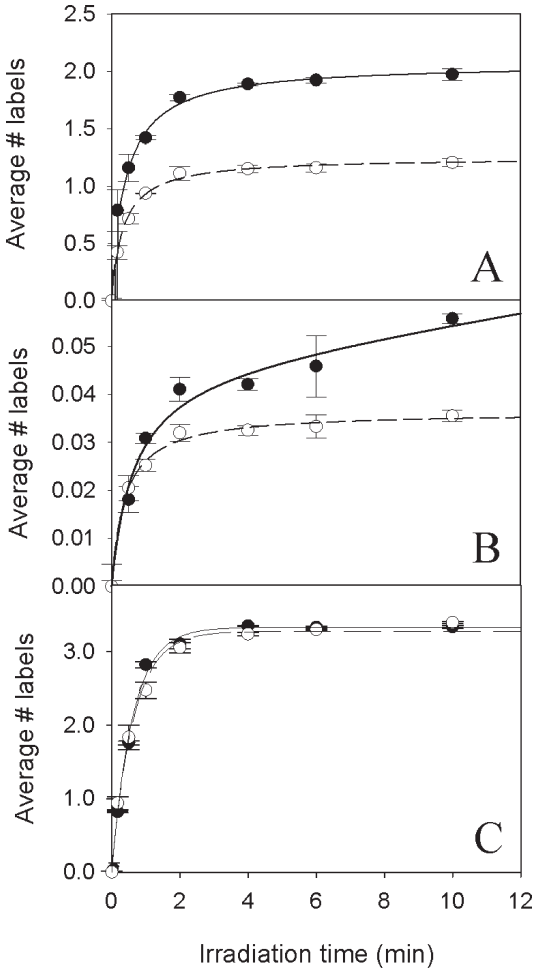

Figure 7. Determining the sensitivity of carbene labeling to ligand binding, for calmodulin-M13 complexation. (A) Free holo-calmodulin (filled circles) is referenced to M13-bound holo-calmodulin (open circles). (B) Free M13 peptide (closed circles) is referenced to bound M13 peptide (open circles). (C) Apo-calmodulin in the absence (closed circles) and presence (open circles) of nonbinding M13 is provided as a control, as apo-calmodulin does not bind M13. Protein and peptide concentrations at 10 μM, using 100 mM photoleucine in Tris buffer. All points represent triplicate analyses, and error bars represent ±1 SD. Lines represent fits for visual clarity.

Effect of Labeling on Structure. To determine if labeling with photoleucine is sensitive to protein conformational changes, ligand binding or both, we first confirmed that labeling for a 2 min period would itself not induce a perturbation of structure in our test proteins. The linear relationship of yield to diazirine concentration in Figure 3a suggests that the labeling event itself does not noticeably alter CaM structure or conformation.[16] In support of this conclusion, we analyzed labeled protein by H/DX-MS immediately following the modification, as H/DX is very sensitive to global conformational change. This analysis returned constant deuterium levels for all labeling levels at complete reagent conversion (Figure 5a,b). Thus, we can conclude the absence of global structural or conformational changes upon labeling for CaM and Mb.

Carbene Labeling Reflects Conformational Change. We then explored if labeling is sensitive to changes in reagent-accessible surface area, brought about by induced protein conformational changes. The conformational change from apo- to holo-CaM served as a test case for this purpose (see Figure S3 in Supporting Information for relevant structures). In biological systems, Ca^{2+} binding to CaM results in the formation of a complex with reduced surface area, capable of regulating biologically relevant protein interactions.[37,38] The resulting differential labeling is shown in Figure 6a. The modification of apo-CaM was 45 ± 7% greater than holo-CaM (calculated over 2−10 min irradiation). This large change in labeling is essentially independent of the buffer system used. The experiment of Figure 6 used a phosphate buffer, whereas a similar experiment in Tris buffer generated a difference of 53 ± 5%.

We note that the maximum yield in phosphate buffer is markedly lower than in Tris buffer, reflecting a reduction in C from 3.2 to 2.2. This supports the concept of reagent surface activity that we introduced above: significant perturbation of labeling would not be expected unless there were an affinity between reagent and protein. The mildly hydrophobic nature of diazirine gas was speculated to introduce a slight enhancement of labeling in regions of greater hydrophobicity.[39] Installing the diazirine moiety on larger chemical structures obviously introduces a greater potential for partitioning at the protein surface based on the chemical nature of the reagent. It is reasonable to

assume photoleucine would not distribute uniformly over the protein surface, as it is a zwitterion at the pH we used, with a nonpolar side chain. A nonuniform distribution would also have implications for the orientation of the diazirine prior to photolysis as well; some may be well positioned for labeling protein and others not. This warrants closer attention and a measure of caution when interpreting carbene labeling data at higher resolution with MS/MS. Studies involving variable pH, ionic strength, and reagent chemistries will determine the degree to which labeling can be targeted to different regions of the protein, but at this stage, it is safe to conclude that photoleucine exhibits less nonselectivity than diazirine gas. A detailed exploration of selectivity will be presented in a future work.

Here, it is worth emphasizing that the large change in labeling upon a simple buffer change did not significantly alter the sensitivity to the CaM conformational change. Exploring the change in greater detail, the calculated increase in SASA is approximately 27%, based on static structures for both apo- and holo-CaM. Increasing the probe size from 1.4 Å to 2.5 Å in these calculations (to better reflect the use of a probe larger than water) reduces surface area but does not change the percent increase in surface area. This imperfect correlation between labeling reduction and SASA is not immediately surprising, as even established methods such as H/D exchange do not correlate well.[40] Here, the nonequivalence could derive in part from the surface activity of the reagent, particularly if it favors a specific subclass of amino acids. However, it should also be stressed that SASA calculations of static structures may themselves be imperfect tools for reflecting reactions that may be influenced strongly by local conformational dynamics. Nonequivalence is also observed for Mb, where the increase in SASA upon extraction of the heme group is estimated at 3% but the labeling changes by 46 ± 7% (Figure 6b).

Carbene Labeling Reflects Protein−Peptide Interactions. We next explored whether carbene labeling is sensitive to structural changes brought about by complexation between a protein and a peptide. The Ca^{2+}-dependent complex formed between holo-CaM and a binding peptide derived from smooth muscle myosin light chain kinase (M13) served as a test case, which has a K_d in the low nanomolar range.[41,42] Figure 7a shows a reduction in labeling for M13-bound CaM of 39 ± 5% with respect to free holo-CaM. M13 also shows a lower level of labeling in the complexed form compared to the free form (Figure 7b). To confirm that reduced labeling arises from the binding event, apo-CaM and M13 were mixed in solution as a noninteracting control, as Ca^{2+} is required for binding. The level of modification was the same for apo-CaM with and without the presence of M13 (Figure 7c) and the labeling of M13 was also unchanged (data not shown).

The calculated reduction in surface area from free to complexed CaM is 3.4%, once again significantly less than the reduction in labeling. The X-ray crystal structure of holo-CaM represents a conformation where the peptide binding site has collapsed. In solution, the average conformational ensemble must be represented by a more open geometry, sufficient to allow peptide incorporation. Sensitivity to both conformational changes and interface formation is a characteristic of all labeling techniques and simply reflects the dynamic nature of protein topography.[43−45]

Single-Pulse Labeling. Because the appearance of labeled protein parallels the conversion of photoleucine to carbene over time, sufficiently high laser pulse energies should provide maximum yield in a single pulse. To test this hypothesis, holo-CaM was labeled with a single pulse in the 20−100 mJ range, as shown in Figure 8. Although these data show scatter arising from to pulse-to-pulse instabilities, the extent of modification increases linearly with pulse energy. Extrapolation suggests that maximum protein labeling at 100 mM photoleucine could be approached within a single ∼600 mJ laser pulse of <10 ns in duration. Q-switched Nd:YAG lasers can meet this requirement. This offers several advantages over integrating protein labeling with a high-frequency laser. First, protein denaturation resulting from the addition of labels would no longer be a concern. Although denaturation was not observed with CaM or Mb, this is not expected to be the case generally. Protein destabilization could occur from the labeling event, as well as from the significant N_2 generated during photolysis. Second, because maximum labeling would arise within the carbene lifetime, tracking *induced* protein unfolding dynamics on the subμs time-scale would be also be possible. Finally, the throughput of the labeling procedure would increase significantly.

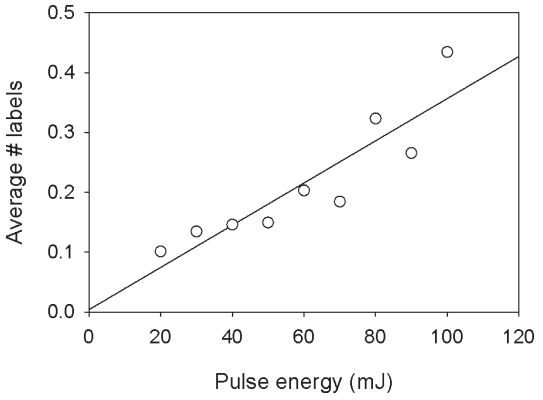

Figure 8. Single-pulse labeling of 10 μM holo-calmodulin with increasing pulse energies, using 100 mM photoleucine in Tris buffer. Scatter plot represents single point analyses.

CONCLUSIONS AND SIGNIFICANCE

This labeling method meets several of the criteria established for an ideal covalent labeling reagent. Labeling is rapid and irreversible, and independent of protein concentration. The diazirine reagent chosen for this study is nonreactive in solution prior to photolysis and may be incorporated as a simple buffer component at moderately high concentrations. Competitive absorption can affect yield in a photon-limited experiment; however, in general the solution conditions for effective labeling permit studies of protein binding or conformational changes. Although carbenes are indiscriminate reactants, our study does suggest a degree of surface bias, deriving from reagent affinity and orientation. This is consistent with a modern view of osmolytes. Additives such as urea, amino acids, and sugars were classically perceived to influence the stability of a protein by altering the water structure at the protein surface.[46] While this remains important in protein stability, surface binding or even exclusionary events are known to occur within osmolyte−protein solutions.[47] A proper study of this selectivity will require additional labeling reagents and future studies will attempt to quantitate the extent of labeling bias through modification patterns of accessible residues. However, we cheerfully note that installing diazirines on variable chemistries may provide a powerful opportunity

to target different chemistries present on proteins, a sort of tunable selectivity. This degree of labeling control would be highly useful in protein footprinting.

■ ASSOCIATED CONTENT

Supporting Information. Additional information as noted in the text. This material is available free of charge via the Internet at http://pubs.acs.org.

■ AUTHOR INFORMATION

Corresponding Author
*Phone: (403) 210-3811. Fax: (403) 283-8727. E-mail: dschriem@ucalgary.ca.

■ ACKNOWLEDGMENT

This work was funded by a Natural Sciences and Engineering Research Council of Canada (NSERC) discovery grant (D.C.S.). D.C.S. holds a Canada Research Chair in Chemical Biology and a Senior Heritage scholarship from Alberta Ingenuity — Health Solutions. We thank Khaled Barakat (Dept. of Physics, University of Alberta) for helping with SASA calculations, and Dr. Yujun Shi (Dept. of Chemistry, University of Calgary) for providing access to the high pulse energy Nd:YAG laser.

■ REFERENCES

(1) Chance, M. *Mass Spectrometry Analysis for Protein-Protein Interactions and Dynamics*; John Wiley & Sons, Inc.: Hoboken, 2008.
(2) Kaltashov, I. A.; Eyles, S. J. *Mass Spectrometry in Biophysics: Conformation and Dynamics of Biomolecules*; John Wiley & Sons: Hoboken, 2005.
(3) Konermann, L.; Tong, X.; Pan, Y. *J. Mass Spectrom.* **2008**, *43*, 1021–1036.
(4) Eyles, S. J.; Kaltashov, I. A. *Methods* **2004**, *34*, 88–99.
(5) Komives, E. A. *Int. J. Mass Spectrom.* **2005**, *240*, 285–290.
(6) Wales, T. E.; Engen, J. R. *Mass Spectrom. Rev.* **2006**, *25*, 158–170.
(7) Kheterpal, I.; Cook, K. D.; Wetzel, R. *Methods Enzymol.* **2006**, *413*, 140–166.
(8) Jørgensen, T. J.; Gårdsvoll, H.; Ploug, M.; Roepstorff, P. *J. Am. Chem. Soc.* **2005**, *127*, 2785–2793.
(9) Zehl, M.; Rand, C. D.; Jensen, O. N.; Jørgensen, T. J. *J. Am. Chem. Soc.* **2008**, *130*, 17453–17459.
(10) Rand, C. D.; Adams, C. M.; Zubarev, R. A.; Jørgensen, T. J. *J. Am. Chem. Soc.* **2008**, *130*, 1341–1349.
(11) Pan, J. X.; Han, J.; Borchers, C. H.; Konermann, L. *J. Am. Chem. Soc.* **2009**, *131*, 12801–12808.
(12) Wang, X.; Kim, S. H.; Ablonczy, Z.; Crouch, R. K.; Knapp, D. R. *Biochemistry* **2004**, *43*, 11153–11162.
(13) Scholten, A.; Visser, N. F.; van den Heuvel, R. H.; Heck, A. J. *J. Am. Soc. Mass Spectrom.* **2006**, *17*, 983–994.
(14) Mailfait, S.; Belaiche, D.; Kouach, M.; Dallery, N.; Chavatte, P.; Formstecher, P.; Sablonniere, B. *Biochemistry* **2000**, *39*, 2183–2192.
(15) Mendoza, V. L.; Vachet, R. W. *Mass Spectrom. Rev.* **2009**, *28*, 785–815.
(16) Mendoza, V. L.; Vachet, R. W. *Anal. Chem.* **2008**, *80*, 2895–2904.
(17) Guan, J. Q.; Chance, M. R. *Trends Biochem. Sci.* **2005**, *30*, 583–592.
(18) Takamoto, K.; Chance, M. R. *Annu. Rev. Biophys. Biomol. Struct.* **2006**, *35*, 251–276.
(19) Kiselar, J. G.; Maleknia, S. D.; Sullivan, M.; Downard, K. M.; Chance, M. R. *Int. J. Radiat. Biol.* **2002**, *78*, 101–114.
(20) Xu, G.; Chance, M. R. *Anal. Chem.* **2004**, *76*, 1213–1221.
(21) Tong, X.; Wren, J. C.; Konermann, L. *Anal. Chem.* **2007**, *79*, 6376–6382.
(22) Tong, X.; Wren, J. C.; Konermann, L. *Anal. Chem.* **2008**, *80*, 2222–2231.
(23) Hambly, D. M.; Gross, M. L. *J. Am. Soc. Mass. Spectrom.* **2005**, *16*, 2057–2063.
(24) Stocks, B. B.; Konermann, L. *Anal. Chem.* **2009**, *81*, 20–27.
(25) Gau, B. C.; Chen, H.; Zhang, Y.; Gross, M. L. *Anal. Chem.* **2010**, *82*, 7821–7827.
(26) Blencowe, A.; Hayes, W. *Soft Matter* **2005**, *1*, 178–205.
(27) Suchanek, M.; Radzikowska, A.; Thiele, C. *Nat. Methods* **2005**, *2*, 261–267.
(28) Richards, F. M.; Lamed, R.; Wynn, R.; Patel, D.; Olack, G. *Protein Sci.* **2000**, *9*, 2506–2517.
(29) Platz, M. In *Carbene Chemistry from Fleeting Intermediates to Powerful Reagents*; Bertrand, G., Ed.; FontisMedia/Lausanne and Marcel Dekker: New York, 2002; pp 27—56.
(30) Craig, P. O.; Ureta, D. B.; Delfino, J. M. *Protein Sci.* **2002**, *11*, 1353–1366.
(31) Gomez, G. E.; Cauerhff, A.; Craig, P. O.; Goldbaum, F. A.; Delfino, J. M. *Protein Sci.* **2006**, *15*, 744–752.
(32) Ureta, D. B.; Craig, P. O.; Gomez, G. E.; Delfino, J. M. *Biochemistry* **2007**, *46*, 14567–14577.
(33) Nuss, J. E.; Alter, G. M. *Protein Sci.* **2004**, *13*, 1365–1378.
(34) McKenna, C. E.; Simeonov, A. M. *Biochemistry* **1996**, *35*, 4502–4514.
(35) Sanner, M. F.; Olson, A. J.; Spehner, J. C. *Biopolymers* **1996**, *38*, 305–320.
(36) Griller, D.; Nazran, A. S.; Scaiano, J. C. *Acc. Chem. Res.* **1984**, *17*, 283–289.
(37) Komeiji, Y.; Ueno, Y.; Uebayasi, M. *FEBS Lett.* **2002**, *521*, 133–139.
(38) Crivici, A.; Ikura, M. *Annu. Rev. Biophys. Biomol. Struct.* **1995**, *24*, 85–116.
(39) Craig, P. O.; Gomez, G. E.; Ureta, D. B.; Caramelo, J. J.; Delfino, J. M. *J. Mol. Biol.* **2009**, *394*, 982–993.
(40) Milne, J. S.; Mayne, L.; Roder, H.; Wand, A. J.; Englander, S. W. *Protein Sci.* **1998**, *7*, 739–745.
(41) Montigiani, S.; Neri, G.; Neri, P.; Neri, D. *J. Mol. Biol.* **1996**, *258*, 6–13.
(42) Bornhop, D. J.; Latham, J. C.; Kussrow, A.; Markov, D. A.; Jones, R. D.; Sorensen, H. S. *Science* **2007**, *317*, 1732–1736.
(43) Wildes, D.; Marqusee, S. *Protein Sci.* **2005**, *14*, 81–88.
(44) Xu, G.; Chance, M. R. *Chem. Rev.* **2007**, *107*, 3514–3543.
(45) Gunasekaran, K.; Ma, B. Y.; Nussinov, R. *Proteins: Struct. Funct. Bioinf.* **2004**, *57*, 433–443.
(46) Tanford, C. *J. Am. Chem. Soc.* **1964**, *86*, 2050.
(47) Rose, G. D.; Fleming, P. J.; Banavar, J. R.; Maritan, A. *Proc. Natl. Acad. Sci. U.S.A.* **2006**, *103*, 16623–16633.